

Electrical and magnetic properties of transition metal oxides $\text{Ln}_{1-x}\text{A}_x\text{MO}_3$ (Ln = Pr, Nd; A = Ca, Sr; M = Mn, Co)

I. G. DEAC*, A. VLĂDESCU, I. BALASZ, A. TUNYAGI, R. TETEAN
Faculty of Physics, Babes-Bolyai University 400084 Cluj-Napoca, Romania

The low temperature electrical and magnetic properties of the polycrystalline perovskite systems $\text{Ln}_{1-x}\text{A}_x\text{MO}_3$ with Ln = Pr, Nd; A = Ca, Sr and M = Mn, Co were studied as a function of the average size of the A-site cations $\langle r_A \rangle$ and of the cation size variance σ^2 . The cobaltites $\text{Pr}_{0.7}\text{A}_{0.3}\text{CoO}_3$ keep some reminiscences of the electrical and magnetic properties of the manganites $\text{Pr}_{0.7}\text{A}_{0.3}\text{MnO}_3$, but they behave differently as a function of the doping ions. Sr substitution for Ca in $\text{Nd}_{0.5}\text{Ca}_{0.5}\text{MnO}_3$ induces FM regions in an AFM background and the phase separation state can be controlled by doping.

(Received March 18, 2010; accepted August 12, 2010)

Keywords: Cobaltites, Manganites, Colossal magnetoresistance, Phase separation, Size variance

1. Introduction

ABO_3 perovskite-type manganites and cobaltites are important for their electronic, magnetic and other properties, as well as for their technical applications [1-3]. The properties of perovskites can be tuned by substituting cations at the A or B sites, or varying the oxygen content. For these type of manganites and cobaltites, doping is needed in order to have the mixed valence $\text{Mn}^{3+}/\text{Mn}^{4+}$ and $\text{Co}^{3+}/\text{Co}^{4+}$ respectively, to induce the desired magnetotransport properties. Mixing cations of different charge at the A sites is the most straightforward experimental method for systematically tuning the properties of these materials. The substitution of divalent alkaline-earth (A = Ca, Sr, Ba, **Pb**) elements for Ln in LnMnO_3 where Ln is a lanthanide, leads to the conversion of Mn^{3+} ($t_{2g}^3e_g^1$ state) into Mn^{4+} ($t_{2g}^3e_g^0$ state) ions. Their spin states do not depend on temperature because the Hund energy is higher than the crystal field energy. Depending on the relative ratio $\text{Mn}^{3+}/\text{Mn}^{4+}$ there is a competition between different interactions: ferromagnetic (FM) double-exchange, antiferromagnetic (AFM) superexchange and Coulomb interaction. This competition gives rise to colossal magnetoresistance (CMR) properties, phase separation, orbital ordering and/or charge ordering (OO/CO) [1,2].

Doped cobaltite perovskites $\text{Ln}_{1-x}\text{A}_x\text{CoO}_3$, have as an unique feature among some other perovskites the change of the Co ions spin-state [3]. In these compounds there are various spin states for trivalent (low-spin LS: $t_{2g}^6e_g^0$; intermediate-spin IS: $t_{2g}^5e_g^1$; high-spin HS: $t_{2g}^4e_g^2$) and tetravalent cobalt ions (LS: $t_{2g}^5e_g^0$; IS: $t_{2g}^4e_g^1$; HS: $t_{2g}^3e_g^2$). The spin-states of undoped LnCoO_3 exhibit a gradual crossover with increasing temperature, from the low-spin (LS) state ($t_{2g}^6e_g^0$) to the intermediate-spin (IS) state ($t_{2g}^5e_g^1$) or to the high-spin (HS) state ($t_{2g}^4e_g^2$). Upon doping A^{2+} ions into LnCoO_3 , some of trivalent Co ions become tetravalent. The Co ion spin states are determined

by the two competing energies, namely, crystal field and Hund coupling, respectively [3].

Perovskite-based structures occasionally show lattice distortion as modifications from the cubic structure due to doping. Rhombohedral, orthorhombic or other lattice distortions result from the tilting and stretching of oxygen octahedra around the transition metal ions. These distortions appear for structural (mismatch of ionic radii) and electronic (Jahn-Teller effect) reasons [1-3].

The magnetotransport properties of these materials have been found to be dependent on internal [4] and external pressure [5], applied magnetic field [6,7], temperature [2], and the chemical composition [8,9] that includes the effects of doping (M oxidation state) [9-11], the average size of the A-site (Ln^{3+} and A^{2+}) cations, $\langle r_A \rangle$ [11,12], and the effect of cation size disparity [13, 14]. The latter is quantified by the variance of the A-cation radius distribution $\sigma^2 = \sum x_i r_i^2 - \langle r_A \rangle^2$ (x_i is the atomic fraction and r_i is the ionic radii of i cation, respectively). The cation size variance describes the effects of disorder due to the disparity or mismatch of individual A cation radii.

When the doping level is kept constant, for the same B-site ion, the decrease of $\langle r_A \rangle$ was found to reduce the M-O-M angle which consequently reduces the energy bandwidth (W) and the critical temperatures for ordering phenomena T_C [2, 13, 14]. The experimental studies on $\text{Ln}_{1-x}\text{A}_x\text{MnO}_3$ compounds have found that the electronic ordering temperatures decrease linearly with σ^2 [13- 15]. The linear dependences of the transition temperatures were attributed to strains resulting from oxygen atom displacements [13-16]. Even control of electronic phase segregation into ferromagnetic and charge ordered AFM regions can be tuned by σ^2 . In addition, these studies indicated that, whatever $\langle r_A \rangle$ and the doping level are, the

increase of σ^2 tends to suppress the magnetic interactions, FM or AFM, and destabilize the CO [15-17].

$\text{Nd}_{0.5}\text{Sr}_{0.5}\text{MnO}_3$ and $\text{Nd}_{0.5}\text{Ca}_{0.5}\text{MnO}_3$ are charged ordered insulators in the ground state [6,18,19]. When $\langle r_A \rangle$ is smaller, as in $\text{Nd}_{0.5}\text{Ca}_{0.5}\text{MnO}_3$, the cooperative Jahn-Teller effect becomes more important than the magnetic interactions, and the material is a charge-ordered insulator without exhibiting ferromagnetism; magnetic fields have no effect on the insulating state of this compound [19]. Increasing σ^2 and $\langle r_A \rangle$ by appropriate substitution, the charge-ordered phase, partially collapses and ferromagnetic clusters can occur, the system showing phase separation, i.e. FM clusters embedded in an AFM matrix. The further increase of σ^2 will result in the depreciation of the ferromagnetic phase, until it disappears completely [20].

The present work is an investigation of the low temperature magnetic properties of two magnetic systems: (1) $\text{Pr}_{0.7}\text{A}_{0.3}\text{MO}_3$ compounds, where A = Ca, Sr and M = Mn or Co (where $\langle r_A \rangle$ and σ^2 are fixed for two values, and B-site ion is changed) and (2) $\text{Nd}_{0.5}\text{Ca}_{0.5-x}\text{Sr}_x\text{MnO}_3$ compounds where both $\langle r_A \rangle$ and σ^2 are changed.

2. Experimental

The $\text{Pr}_{0.7}\text{Ca}_{0.3}\text{MnO}_3$, $\text{Pr}_{0.7}\text{Ca}_{0.3}\text{CoO}_3$, and $\text{Pr}_{0.7}\text{Sr}_{0.3}\text{CoO}_3$ and $\text{Nd}_{0.5}\text{Ca}_{0.5-x}\text{Sr}_x\text{MnO}_3$ ($x = 0, 0.05, 0.1, 0.25, 0.4, 0.5$) compounds were prepared by conventional solid state reactions at high temperatures.

The powder x-ray diffraction patterns were recorded by using a Bruker D8 Advance AXS diffractometer with Cu $K\alpha$ radiation. Data were refined by the Rietveld method using the program FULLPROF. A cryogen free VSM magnetometer (Cryogenic Ltd.) was used for magnetization and ac susceptibility measurements in the temperature range 5 - 300 K and up to 12 T. The temperature dependent magnetization, $M(T)$, was recorded in two modes. In the ZFC mode, the sample was first cooled to $T = 5$ K in zero field and data were taken while warming after establishing a magnetic field at 5 K. In field-cooled (FC) mode, the field was applied at 300 K, and data were taken during warming, in a field. The resistivities were measured in a cryogen free magnet cryostat CFM-7 T (Cryogenic Ltd.) by the four-probe technique, in the temperature range from 5 to 300 K and magnetic fields up to 7 T.

3. Results and discussions

The X-ray diffraction patterns for all the studied samples showed the presence of a single phase. The Pr-based samples have perovskite structure with orthorhombic $Pbnm$ symmetry. The same type of symmetry was found for the Nd series. The unit cell parameters are in close agreement with the values reported in earlier works [4, 21-24].

In Fig. 1 we describe the temperature dependence of the FC and ZFC magnetization for the $\text{Pr}_{0.7}\text{Ca}_{0.3}\text{MnO}_3$ compound. The magnetization has a history dependence with a bifurcation between zero field cooling (ZFC) and field cooling (FC) data at an irreversibility temperature T_{irr} . This sample was found to have charge ordering phase (CO) below 250 K, then it became an antiferromagnetic (AFM) insulator at about 130 K. Below 110 K it has ferromagnetic-like behavior [21,22].

At lower temperatures, below 110 K the inverse dc susceptibility $\chi(T)$ deviates upward from a Curie-Weiss prediction, as shown in the inset of Fig. 1. This ferromagnetic (FM) phase is not a genuine one but it consists in ferromagnetic clusters embedded in an antiferromagnetic matrix [25].

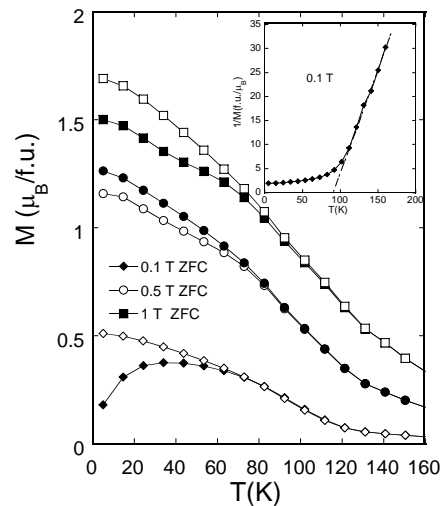


Fig. 1. Field cooled (open symbols) and zero field cooled (closed symbols) magnetizations of $\text{Pr}_{0.7}\text{Ca}_{0.3}\text{MnO}_3$ as a function of temperature. In inset the reciprocal magnetization taken in 0.1 T is shown.

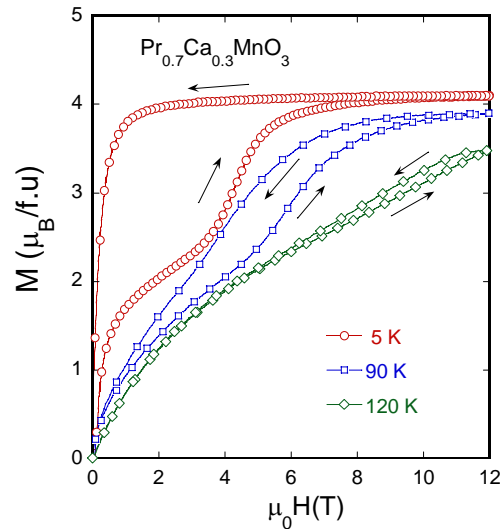


Fig. 2. $M(H)$ curves for the sample $\text{Pr}_{0.7}\text{Ca}_{0.3}\text{MnO}_3$ taken at 5 K, 90 K and 120 K.

The coexistence of the two phases can be seen from Fig. 2, in $M(H)$ curves at low temperatures where a metamagnetic transition occurs, suggesting the phase separation. i.e. the presence of both FM and AFM phases in the sample. We can estimate the volume fraction which is ferromagnetic after zero-field cooling (f_{FM}) by taking the ratio of the metamagnetic transition magnetization to the theoretically expected magnetization ($3.67\mu_B/f.u.$) for complete alignment of all the Mn moments. It can be seen from Fig. 2 that f_{FM} is higher than 65% below 90 K.

$Pr_{0.7}Ca_{0.3}MnO_3$ is insulator below 4 T on the whole temperature range [21, 22]. In this compound the average cation radius is $\langle r_A \rangle = 1.305 \text{ \AA}$ and the variance $\sigma^2 = 5.25 \cdot 10^{-4} \text{ \AA}^2$, presuming that the perovskite A-site is coordinated by 12 O^{2-} ions [3, 26].

If we keep the same $\langle r_A \rangle$ and σ^2 , but the B-site element is Co, the electrical and magnetic properties are different from those of $Pr_{0.7}Ca_{0.3}MnO_3$.

In Fig. 3, the magnetic behavior of $Pr_{0.7}Ca_{0.3}CoO_3$ is described. This compound shows, again, different behavior in ZFC and FC modes. The temperature dependence of the inverse magnetization $M^{-1}(T)$ has a linear dependence at high temperatures, but it has now a downward deviation at a temperature $T_G \sim 40$ K, suggesting the occurrence of a Griffiths phase [27]. This means that the short-range FM phases are formed above T_C . The T_C is estimated as the inflection point of the $M(T)$ curve and $T_C \sim 25$ K. In the Griffiths phase, there is no interaction between the short-range FM clusters, which means that these clusters are separated and disordered.

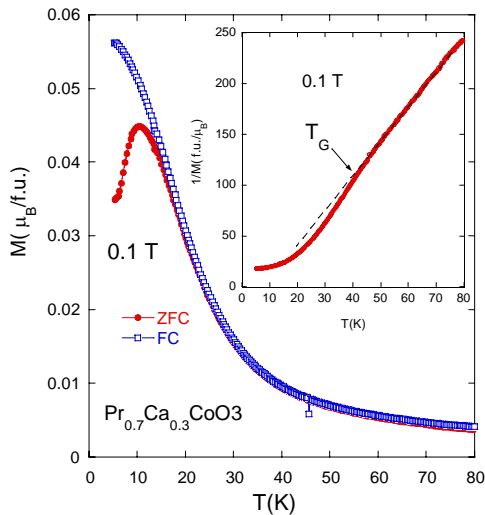


Fig. 3. Field cooled and zero field cooled magnetizations of $Pr_{0.7}Ca_{0.3}CoO_3$ as a function of temperature. In inset the temperature dependence of reciprocal magnetization taken in 0.1 T is shown.

A frequency dependent maximum of the real part of the ac susceptibility $\chi'(T)$ was found at low temperatures, as can be seen in Fig. 4. All these features indicate the

presence of magnetic disorder in the system. This spin disorder is supposed to be created by the presence of hole-rich and hole-poor regions due to the spin state transitions of Co^{3+} and Co^{4+} ions [3].

The magnetic disorder has a strong influence on the scattering processes, increasing the magnitude of the resistivity $\rho(T)$ that has a semiconducting behavior (Fig. 7). A small negative magnetoresistance $MR = [\rho(H) - \rho(0)]/\rho(0)$ of about 2 % (at 7 K) was found in a magnetic field of 7 T.

While for the sample with $M = Mn$ we found FM clusters embedded in a AFM matrix, when $M = Co$ no AFM phase was found in $Pr_{0.7}Ca_{0.3}CoO_3$ and we presume that the spin disorder is generated by the multitude of the possible spin states of Co ions.

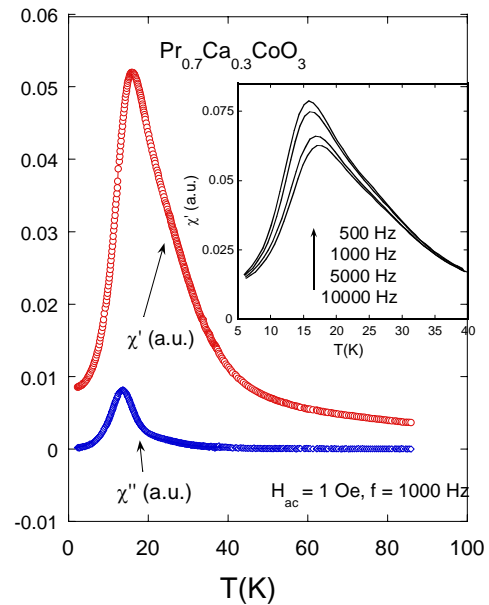


Fig. 4. Real (χ') and imaginary (χ'') components of the ac susceptibility of $Pr_{0.7}Ca_{0.3}CoO_3$ measured in zero applied static magnetic field. $H_{ac} = 1Oe$ and $f = 1000$ Hz. In inset: frequency dependence of $\chi'(T)$.

If we replace the doping element Ca by Sr, keeping the same ratio ($Pr_{0.7}Sr_{0.3}$), the average cation radius increases to $\langle r_A \rangle = 1.335 \text{ \AA}$ and the size variance becomes $\sigma^2 = 4.725 \cdot 10^{-3} \text{ \AA}^2$. $Pr_{0.7}Sr_{0.3}MnO_3$ has a ferromagnetic-paramagnetic transition at about $T_C \sim 250$ K accompanied by an metal-insulator (MI) transition very close to this temperature [28,29]. A negative magnetoresistance MR of about 80% (at 250 K) was found for this sample in 8 T [28,29].

In the similar cobaltite compound $Pr_{0.7}Sr_{0.3}CoO_3$ we found ferromagnetic behaviour below 190 K as shown in Fig. 5 and bifurcation of magnetization $M(T)$ curves taken in FC and ZFC modes.

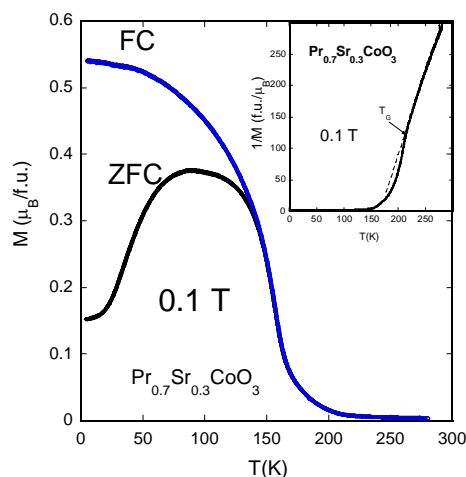


Fig. 5. Field cooled and zero field cooled magnetizations of $\text{Pr}_{0.7}\text{Sr}_{0.3}\text{CoO}_3$ as a function of temperature. In inset the thermal dependence of reciprocal magnetization taken in 0.1 T is shown.

The temperature dependence of the inverse magnetization $M^{-1}(T)$ has the typical shape that indicates the presence of a Griffiths phase, i.e. a downward deviation from the Curie-Weiss dependence. T_G is about 220 K and it has no magnetic field dependence. A frequency dependent cusp (not shown) of the real part of the ac susceptibility $\chi'(T)$ was found in the region of the transition for this compound. No saturation was seen in $M(H)$ dependencies up 12 T as shown in Fig. 6.

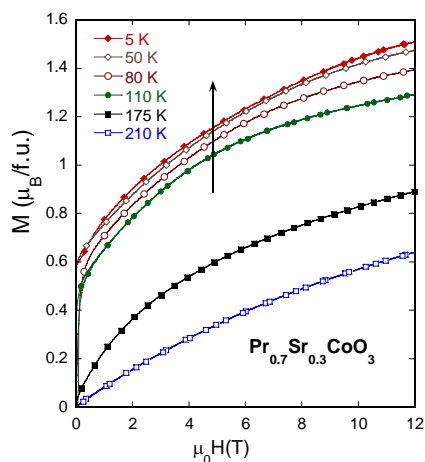


Fig. 6. Magnetization vs field measured at various temperatures for sample $\text{Pr}_{0.7}\text{Sr}_{0.3}\text{CoO}_3$.

These results indicate again the presence of the magnetic disorder in the system, generated probably by the randomly distributed Co ions in various spin states. This phase is characterized by the coexistence of ferromagnetic

entities within the globally paramagnetic phase far above the magnetic ordering temperature.

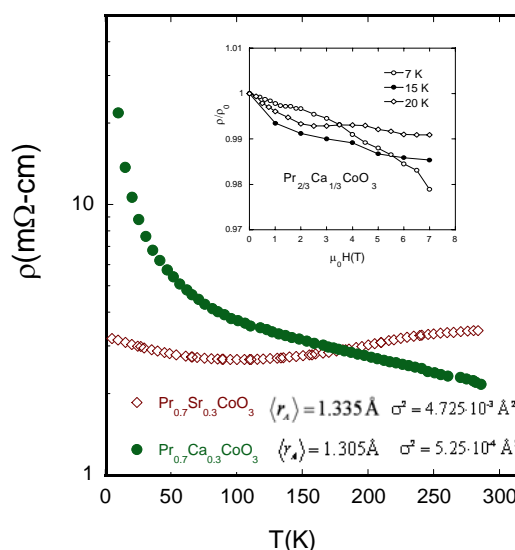


Fig. 7. Temperature dependence of the resistivity for the samples $\text{Pr}_{0.7}\text{Sr}_{0.3}\text{CoO}_3$ and $\text{Pr}_{0.7}\text{Ca}_{0.3}\text{CoO}_3$ on cooling in zero magnetic field. In inset: thermal dependence of ρ/ρ_0 .

The temperature dependence of the electrical resistivity $\rho(T)$ has metallic behavior with a small feature (a change of slope) at the transition temperature, as described in Fig.7. Negligible magnetoresistance was found in this sample. The upturn in $\rho(T)$ at low temperatures was attributed to grain boundary effects that occur in polycrystalline samples [27]. The effect of the average cation radius and of the variance on the resistivity of the two cobaltite samples is shown in Fig.7. The bigger Sr ion makes the compound more metallic, by means of a better overlapping of the Co and O orbitals [24].

While in the manganites $\text{Pr}_{0.7}\text{A}_{0.3}\text{MnO}_3$ the ground state is either a pure ferromagnetic phase when A = Sr or a phase separated one like in the case A = Ca, the corresponding formula cobaltites show a transition in a non long-range ferromagnetic phase by means of a Griffiths phase.

The other series of compounds $\text{Nd}_{0.5}\text{Ca}_{0.5-x}\text{Sr}_x\text{MnO}_3$ has the average cationic radius between $\langle r_A \rangle = 1.305 \text{ \AA}$ (identical with that of Pr-Ca samples) for $x = 0$, and $\langle r_A \rangle = 1.355 \text{ \AA}$ for $x = 0.5$. The size variance changes from $\sigma^2 = 1.225 \cdot 10^{-3} \text{ \AA}^2$ to $\sigma^2 = 7.225 \cdot 10^{-3} \text{ \AA}^2$, respectively.

$\text{Nd}_{0.5}\text{Ca}_{0.5}\text{MnO}_3$ is a typical charge-ordered manganite which shows CO around 240 K and antiferromagnetic ordering (CE-type) at lower temperatures ($\sim 150 \text{ K}$). The magnetic behavior of this compound is illustrated in Figs. 8 and 9.

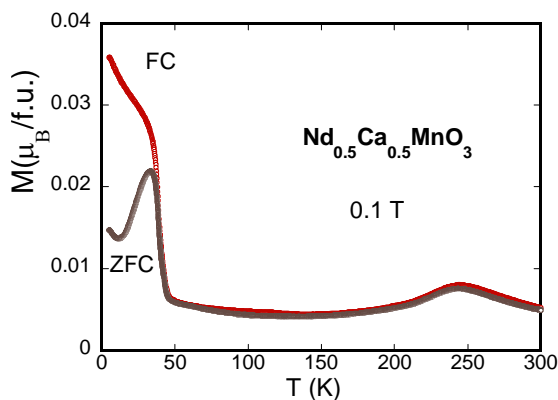


Fig. 8. Field cooled (FC) and zero field cooled (ZFC) magnetization as a function of temperature for the sample $Nd_{0.5}Ca_{0.5}MnO_3$ measured in 0.1 T.

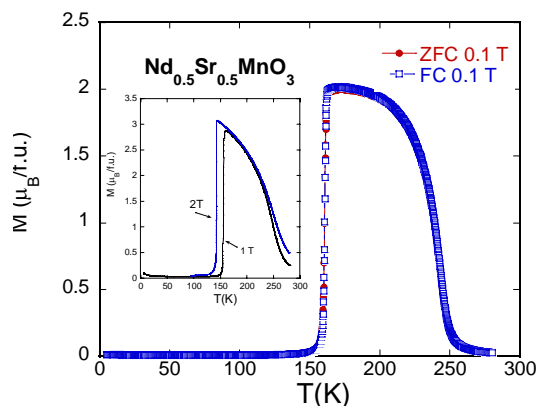


Fig. 10. Field cooled (FC) and zero field cooled (ZFC) magnetization as a function of temperature for the sample $Nd_{0.5}Sr_{0.5}MnO_3$ measured in 0.1 T. In inset: magnetization vs temperature measured in 1 and 2 T.

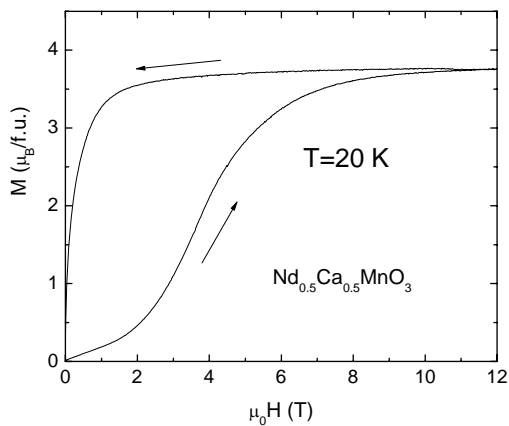


Fig. 9. Magnetization vs field measured at 20 K for sample $Nd_{0.5}Ca_{0.5}MnO_3$.

Some irreversibility occurs and FC and ZFC curves deviate from each other. The low temperature increase of magnetization is attributed to paramagnetic Nd ions and to the weak Mn-Nd interaction [31].

No trace of ferromagnetic phase was seen in this compound by high frequency electron spin resonance (ESR) [31], in low applied magnetic fields. A high magnetic field can induce ferromagnetic behavior in the sample after a metamagnetic transition, as shown in Fig. 9. The compound remains insulating whatever the temperature.

The other end series compound $Nd_{0.5}Sr_{0.5}MnO_3$ is ferromagnetic below ~ 260 K and it shows CO at lower temperatures (~ 150 K) accompanied by antiferromagnetism (CE-type) [32]. In higher magnetic field, the ferromagnetic phase extends to lower temperatures. This behavior is described in Figs. 10 and 11, our data being in agreement with prior reports [32].

In this case we found a negligible irreversibility in ZFC and FC magnetization curves but a hysteresis occurs in high magnetic field $M(H)$ curves below 150 K as shown in Fig. 11. Here again, the CO state can be “melted” by a high magnetic field. No ferromagnetic phase was seen below 150 K in zero applied magnetic field.

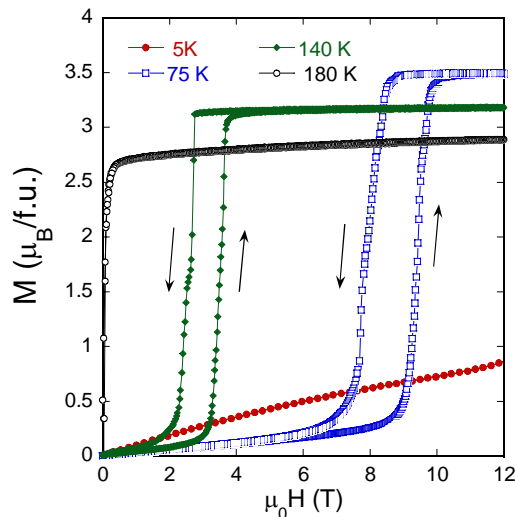


Fig. 11. Magnetization vs field measured at 20 K for sample $Nd_{0.5}Ca_{0.5}MnO_3$.

The magnetic properties of the $Nd_{0.5}Ca_{0.5}MnO_3$ change dramatically when Sr substitutes for Ca in this compound. As it can be seen in Fig. 12 the magnetization of the system increases when Sr replaces Ca, due to a ferromagnetic component that occurs in the sample at low temperatures.

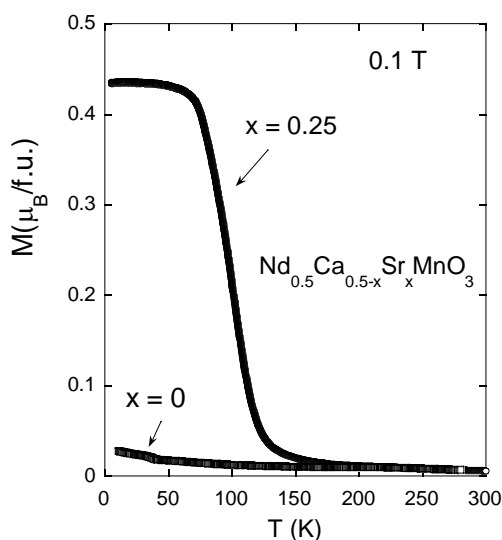


Fig. 12. Field cooled magnetization as a function of temperature measured in 0.1 T for the samples with $x = 0$ and $x = 0.25$ of the system $\text{Nd}_{0.5}\text{Ca}_{0.5-x}\text{Sr}_x\text{MnO}_3$.

The fraction of the FM component in the AFM matrix can be estimated from high field $M(H)$ measurements, as described in Fig. 13 for the sample with $x = 0.25$. The volume fraction which is ferromagnetic after zero-field cooling was estimated in the same way as we did it for the Pr-based manganites using a theoretically expected magnetization of $3.5 \mu_B/\text{f.u.}$ for complete alignment of all the Mn moments.

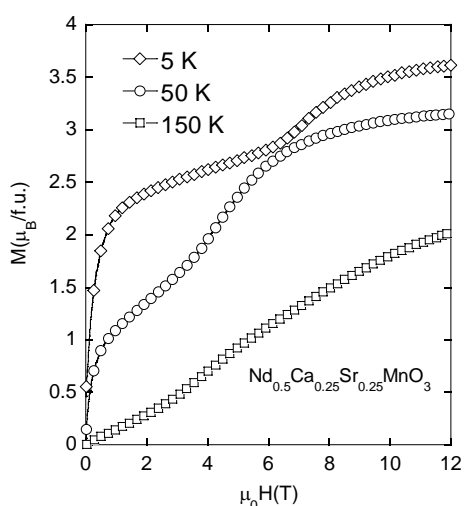


Fig. 13 Magnetization vs field measured at various temperatures for sample $\text{Nd}_{0.5}\text{Ca}_{0.25}\text{Sr}_{0.25}\text{MnO}_3$.

In Fig. 14 we show the dependence of the FM fraction in the $\text{Nd}_{0.5}\text{Ca}_{0.5-x}\text{Sr}_x\text{MnO}_3$ system on the Sr content taken at 5 K and 20 K. The FM component of the samples grows with Sr content to reach a maximum and then it goes to zero as x approaches the value $x = 0.5$.

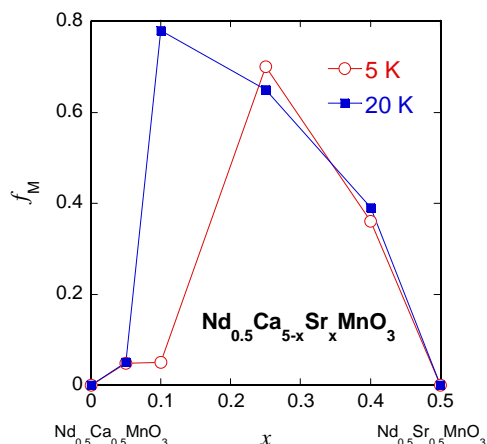


Fig. 14. The volume fraction of ferromagnetic phase at 5 K and 20 K (from $M(H)$ data as described in the text).

A similar effect was found by D. Zhu *et al.* in $\text{Nd}_{0.5}\text{Ca}_{0.5-x}\text{Ba}_x\text{MnO}_3$ [33]. They found that the FM fraction first quickly increases with x reaches a maximum value of 26% for $x=0.03$, and then slowly decreases as more Ba is introduced. The explanation they gave [33,34], can also be adapted for the $\text{Nd}_{0.5}\text{Ca}_{0.5-x}\text{Sr}_x\text{MnO}_3$ system. In half-doped manganites, the Jahn-Teller effect leads to the occurrence of the strongly distorted $\text{Mn}^{3+}-\text{O}_6$ octahedra (where we have not a perfect overlapping of the Mn and O orbitals) that alternate with much less distorted $\text{Mn}^{4+}-\text{O}_6$ octahedra. This arrangement is responsible for the AFM and insulating nature of these CO compounds [1,2]. Replacing Ca^{2+} ion by the larger Sr^{2+} ion (increasing the A-site cation radius) the distortion of the $\text{Mn}^{3+}-\text{O}_6$ octahedra is reduced. In this way, more symmetric domains will develop around the Sr^{2+} allowing a better overlapping of the Mn and O orbitals, and this will result in the formation of small FM domains [31,32]. This is the so-called ‘counter-distortion’ effect [34]. An other interesting aspect is that, the increase of the A-site cationic size mismatch, i.e. of the variance σ^2 , destroys the FM phase and this will become favorable for AFM phase growing. As it can be seen in Fig. 14, the FM fraction f_{FM} increases until a maximum value, with the Sr content x , and then it goes to zero as the variance becomes too high. This suggests a competition between the ‘counter-distortion’ effect and the effect of the size variance. As shown in Fig. 14, the ferromagnetic fraction depend not only on Sr content but it is also temperature dependent, probably due to the temperature induced changes on the lattice and on the correlated local lattice distortions [34-36].

4. Conclusions

The low temperature properties of the polycrystalline perovskite systems $\text{Ln}_{1-x}\text{A}_x\text{MO}_3$ with Ln = Pr, Nd; A = Ca, Sr and M = Mn, Co including electrical resistance, magnetization and ac susceptibility were studied. These properties were found to be strongly dependent on the the

average size of the A-site (Ln^{3+} and A^{2+}) cations $\langle r_A \rangle$ and on the cation size variance σ^2 . The analysis indicate that the cobaltites $\text{Pr}_{0.7}\text{A}_{0.3}\text{CoO}_3$ keep some reminiscences of the electrical and magnetic properties of their corresponding formula manganites $\text{Pr}_{0.7}\text{A}_{0.3}\text{MnO}_3$, but they behave differently as a function of the doping ions. While the preformed clusters above Curie temperature, in these cobaltites have the characteristics of a Griffith phase, in $\text{Pr}_{0.7}\text{A}_{0.3}\text{MnO}_3$ this model is not applicable. The systematic analysis of $\text{Nd}_{0.5}\text{Ca}_{0.5-x}\text{Sr}_x\text{MnO}_3$ indicate that Sr substitution for Ca induces FM regions in an AFM background. The ratio of the magnetic components of this phase separation state can be controlled by doping. The FM fraction increases with x, reaching a maximum, and then it decreases as the A-site mismatch becomes to high.

Acknowledgments

This work was supported by the grant IDEI 2590 of CNCSIS, Romania.

References

- [1] J. M. D. Coey, M. Viret, S. von Molnar, *Adv. Phys.* **48**, 167 (1999).
- [2] Y. Tokura, *Rep. Prog. Phys.* **69**, 797 (2006).
- [3] M. A. Señarís-Rodríguez, J. B. Goodenough, *J. Solid State Chem.* **118**, 323 (1995).
- [4] C. N. R. Rao, P. N. Santhosh, R. S. Singh, A. Arulraj, *J. Solid State Chem.* **135**, 169 (1998).
- [5] H. Y. Hwang, T. T. M. Palstra, S.-W. Cheong, B. Batlogg, *Phys. Rev. B* **52**, 15046 (1995).
- [6] A. Asamitsu, Y. Moritomo, Y. Tomioka, T. Arima, Y. Tokura, *Nature* **373**, 407 (1995).
- [7] H. Kuwahara, Y. Tomioka, A. Asamitsu, Y. Moritomo, Y. Tokura, *Science* **270**, 961 (1995).
- [8] P. Schiffer, A. P. Ramirez, W. Bao, S.-W. Cheong, *Phys. Rev. Lett.* **75**, 3336 (1995).
- [9] R. Mahendiran, R. Mahesh, A. K. Raychaudhuri, C. N. R. Rao, *Solid State Communications*, **94**, 515 (1995).
- [10] R. Mahesh, R. Mahendiran, A. K. Raychaudhuri, C. N. R. Rao, *J. Solid State Chem.* **120**, 204 (1995).
- [11] R. Mahesh, R. Mahendiran, A. K. Raychaudhuri, C. N. R. Rao, *J. Solid State Chem.* **114**, 297 (1995).
- [12] P. G. Radaelli, M. Marezio, H. Y. Hwang, S.-W. Cheong, *J. Solid State Chem.* **122**, 444 (1996).
- [13] J. P. Attfield, *International Journal of Inorganic Materials* **3**, 1147 (2001).
- [14] J. P. Attfield, *Crystal Engineering* **5**, 427 (2002).
- [15] L. M. Rodríguez-Martínez, H. Ehrenberg, J. Paul Attfield, *Solid State Sciences* **2**, 11 (2000).
- [16] L.M. Rodríguez-Martínez, J.P. Attfield, *Phys. Rev. B* **54**, 15622 (1996).
- [17] F. Damay, C. Martin, A. Maignan, B. Raveau, *J. Appl. Phys.* **82**, 6181, (1997).
- [18] R. Kajimoto, H. Yoshizawa, H. Kawano, H. Kuwahara, Y. Tokura, K. Onoyama, M. Ohashi, *Phys. Rev. B* **60**, 9506 (1999).
- [19] F. Millange, S. de Brion, G. Chouteau, *Phys. Rev. B* **62**, 5619 (2000).
- [20] B. Raveau, *Phil. Trans. R. Soc. A* **366**, 83 (2007).
- [21] H. Yoshizawa, H. Kawano, Y. Tomioka, Y. Tokura, *J. Phys. Soc. Jpn.* **65**, 1043 (1996).
- [22] Y. Tomioka, A. Asamitsu, H. Kuwahara, Y. Moritomo, Y. Tokura, *Phys. Rev. B* **53**, R1689 (1996).
- [23] A. K. Kundu, E.V. Sampathkumaran, K. V. Gopalakrishnan, C. N. R. Rao, *J. Magn. Mater.* **281**, 261 (2004).
- [24] C. Leighton, D. D. Stauffer, Q. Huang, Y. Ren, S. El-Khatib, M. A. Torija, J. Wu, J. W. Lynn, L. Wang, N. A. Frey, H. Srikanth, J. E. Davies, Kai Liu, J. F. Mitchell, *Phys. Rev. B* **79**, 214420 (2009).
- [25] I. G. Deac, J. F. Mitchell, P. Schiffer, *Phys. Rev. B* **63**, 172408 (2001).
- [26] R. D. Shannon, *Acta Crystallogr. A* **21**, 751 (1976).
- [27] M. B. Salamon and S. H. Chun *Phys. Rev. B* **68**, 014411 (2003).
- [28] J. G. Park, M. S. Kim, H.-C. Ri, K. H. Kim, T. W. Noh, S.-W. Cheong, *Phys. Rev. B* **60**, 14804 (1999).
- [29] N. Rama, V. Sankaranarayan, M. S. Ramachandra Rao, *J. All. Comp.* **466**, 12 (2008).
- [30] M. Ziese, *Rep. Prog. Phys.* **65**, 143 (2002).
- [31] F. Dupont, F. Millange, S. de Brion, A. Janossy, G. Chouteau, *Phys. Rev. B* **64**, 220403 (2001).
- [32] H. Kuwahara, Y. Tomioka, A. Asamitsu, Y. Moritomo, Y. Tokura, *Science* **270**, 961 (1995).
- [33] D. Zhu, P. Cao, W. Liu, X. Ma, A. Maignan, B. Raveau, *Materials Letters* **61**, 617 (2007).
- [34] B. Raveau, *Phil. Trans. R. Soc. A* **366**, 83 (2007).
- [35] K. Liu, X. W. Wu, K. H. Ahn, T. Sulchek, C. L. Chien, J. Q. Xiao, *Phys. Rev. B* **54**, 3007 (1997).
- [36] V. Kiryukhin, B. G. Kim, T. Katsufuji, J. P. Hill, S.-W. Cheong, *Phys. Rev. B* **63**, 144406 (2001).

*Corresponding author. ideac@phys.ubbcluj.ro